Society For Biomaterials

Biological response of endothelial cells to diamond-like carbon-coated NiTi alloy

Ruiqiang Hang,[1] Ming Zhang,[1] Shengli Ma,[1] Paul K. Chu[2]

[1]State Key Laboratory for Mechanical Behavior of Materials, Xi'an Jiaotong University, Xi'an 710049, China
[2]Department of Physics and Materials Science, City University of Hong Kong, Tat Chee Avenue, Kowloon, Hong Kong, China

Received 27 April 2011; revised 11 July 2011; accepted 26 September 2011
Published online 29 November 2011 in Wiley Online Library (wileyonlinelibrary.com). DOI: 10.1002/jbm.a.33295

Abstract: Diamond-like carbon (DLC) coatings were deposited on nearly equiatomic nickel-titanium (NiTi) alloy by arc-enhanced magnetron sputtering. The microstructure, surface morphology, chemical composition, surface free energy, protein adsorbance, and leach amount of Ni ions were assessed by Raman spectroscopy, high-resolution transmission electron microscopy (HR-TEM), atomic force microscopy (AFM), X-ray photoelectron spectroscopy (XPS), contact angle measurements, micro BCA^{TM} protein assay kit, and inductively coupled plasma mass spectrometry (ICP-MS). The biological response of the endothelial cells (ECs) was evaluated by cell adhesion, morphology, viability, and expression levels of thrombogenicity-related genes. Our results show that the DLC coatings inhibit the release of Ni ions from the NiTi substrate effectively thus enhancing its biosafety. The easy adhesion, elongated morphology, and high viability of ECs on the DLC coatings suggest fast endothelialization after implantation and so application of DLC coatings improves the surface properties of NiTi in cardiovascular applications. The relationship between the surface characteristics, Ni leaching, and concomitant biological response are discussed in details. © 2011 Wiley Periodicals, Inc. J Biomed Mater Res Part A: 100A: 496–506, 2012.

Key Words: diamond-like carbon, nickel-titanium alloy, endothelial cells, biological response

How to cite this article: Hang R, Zhang M, Ma S, Chu PK. 2012. Biological response of endothelial cells to diamond-like carbon-coated NiTi alloy. J Biomed Mater Res Part A 2012:100A:496–506.

INTRODUCTION

The blood circulatory system composed of the heart, blood, and blood vessels is vital to human health,[1] but unfortunately, cardiovascular diseases are more prevalent nowadays because of unhealthy lifestyle and aging.[2] Interventional treatment is a minimally invasive treatment that is particularly effective for cardiovascular diseases such as atherosclerosis or coronary artery disease.[3] In the interventional treatment, the stents are inserted in a collapsed state into blood vessels and stretched open to enlarge the pathological vessel. Stents made of NiTi alloy have attracted much attention because of its shape memory effect and superelasticity. They not only fit the vascular lumen tightly after deployment, but also offer constant stress over a wide range of strain to maintain the lumen diameter consequently minimizing vascular damage.[4] The serious problem associated with bare metal stents (BMS) is restenosis induced by neointimal hyperplasia after deployment because of the excessive proliferation of smooth muscle cells (SMCs). As a result, drug-eluting stents (DES) have emerged to reduce the restenosis rate by depressing the proliferation of SMCs, but recent studies indicate increased risk of late stent thrombosis because of the inhibition of proliferation of endothelial cells (ECs) by drugs simultaneously.[5,6] Failure of DES has led researchers to pay more attention to surface-modified BMS for rapid endothelialization. It has been reported that rapid coverage by an endothelial monolayer not only can inhibit the formation of thrombus, but also can prevent proliferation of SMCs.[7] On the other hand, although NiTi alloys have been used clinically in recent years, long-term is still a concern due to leaching of toxic nickel ions. The human body fluid is a complex electrochemical system which can corrode metallic implants *in vivo* after surgical insertion degrading the mechanical properties and expedites Ni release from the implants. It has been reported that the amount of leached Ni ions increases with time and remains at a high level after implantation for 8 weeks or even several months.[8–11] Excessive Ni ions may suppress cell metabolism, differentiation, and proliferation and induce cell apoptosis as well as carcinogenic consequence.[12,13] Moreover, exposure of ECs to Ni-containing surface may increase the oxidative stress to pathological levels in cells.[4] Hence, the proper use of surface modification to inhibit the release of Ni ions from the bulk materials and minimize the surface Ni contents on NiTi alloys is important.

Correspondence to: S. Ma; e-mail: slma@mail.xjtu.edu.cn
Contract grant sponsor: Joint Project of Guangdong Province and Ministry of Education of China; contract grant number: 2007A090302087
Contract grant sponsor: Hong Kong Research Grants Council (RGC) General Research Funds (GRF); contract grant number: CityU 112510

Surface oxidation is a common method to enhance the biocompatibility of NiTi alloys,[4,14–16] but as Shabalovskaya[16] reported, the formed oxide film after long-term implantation might not be safe even it had a small Ni concentration and the Ni-rich sublayer might serve as a Ni reservoir leading to prolonged Ni release. Diamond-like carbon (DLC) coatings which can be readily deposited on a myriad of materials by physical and chemical vapor deposition[17] have excellent mechanical properties, corrosion resistance, and blood compatibility. Using the proper deposition technique and parameters, the strain when 1% delamantion occurs on the DLC coatings on NiTi alloy can reach 10% which is greater than normally encountered strain.[18] Compared to the bare NiTi alloy, the DLC coatings can reduce the amounts of released Ni to much smaller.[19] For example, after 6 months of immersion, the amount of leached Ni ions from the DLC-coated sample was reported to be over one-sixth of that from bare NiTi alloy[20] corroborating the ability of DLC to block Ni out-diffusion. The pitting potential of DLC-coated NiTi increases by five folds[19,21] and this factor may be responsible for the reduced long-term Ni release. Moreover, the number of adhered and activated platelets is significantly reduced and the adsorption ratio of albumin to fibrinogen increases,[9] signifying improved blood compatibility. However, since endothelialization is crucial to cardiovascular implants, the biological response of ECs to DLC coatings is important and needs systematic investigation. The objective of this study is to investigate the biological response of ECs on DLC coatings deposited on NiTi alloy by arc-enhanced magnetron sputtering (AEMS).

MATERIALS AND METHODS

Sample preparation

Arc-enhanced magnetron sputtering (AEMS) was used to deposit DLC coatings onto polished nearly equiatomic nickel-titanium (50.7 at% Ni) alloy sheets with dimensions of 15 mm $\times$ 15 mm $\times$ 2 mm. The substrates were ultrasonically washed with acetone, alcohol, and distilled water for 15 min sequentially and then dried in a nitrogen atmosphere before introduction into the columnar deposition chamber with a diameter of 900 mm and height of 600 mm. A columnar titanium target with a diameter of 60 mm and height of 450 mm produced the arc discharge with a hollow and permanent magnet placed in the center of the hole. Ultra-pure graphite targets (two pairs of targets with dimensions of 435 mm $\times$ 94 mm $\times$ 8 mm) were used to prepare the DLC coatings. The substrates were rotated at a speed of 10 rpm during sputter cleaning and deposition. After the chamber was evacuated to a base pressure of 6.0×10^{-3} Pa by mechanical and molecular pumps, the heating system in the center of the chamber was turned on. After the temperature reached 150°C, argon plasma was triggered to bombard the substrates for 30 min at a bias voltage of -1 kV and pressure of 4 Pa to remove undesirable surface oxide and contamination. A Ti interlayer was first deposited using the columnar Ti target (operated at 20 V and 60 A) at 0.3 Pa in the arc discharge mode for 5 min to improve the adhesion between the substrates and coatings. Afterward, the DLC films were deposited using a pulsed DC bias voltage of -100 V, duty factor of 40%, pulse frequency of 40 kHz, graphite target power of 3 kW, chamber temperature of 150°C, working pressure of 0.3 Pa (argon flow rate of 24 sccm), and deposition time of 60 min.

Microstructure and surface characterization

Raman spectroscopy (Almega) was performed to investigate the chemical characteristics of the carbon films. The Raman spectra were excited by a 532 nm argon ion laser with a power of 25 mW at room temperature. The spectra in the range of 900–1800 cm^{-1} were fitted using the Gaussian/Lorentzian (G/L = 4.0) distribution. High-resolution transmission electron microscopy (HR-TEM, JEM-200CX at 200 kV) was used to observe the atomic structure of the carbon films. The surface morphology of the substrate and coating was characterized by atomic force microscopy (AFM, Agilent Picoplus) in the contact mode under ambient conditions.

To evaluate the chemical bonding of NiTi alloy and DLC coatings, X-ray photoelectron spectroscopy (XPS, Axis Ultra, Kratos, UK) with monochromatic Al Kα radiation (150 W, 15 kV, 1486.6 eV) was performed. The survey spectra were obtained at constant pass energy of 160 eV and high-resolution Ni 2p, Ti 2p, C 1s, O 1s, and N 1s spectra were recorded at constant pass energy of 80 eV. The binding energies were calibrated relative to the C 1s peak (284.8 eV) from adsorbed hydrocarbons on the surface. The high-resolution spectra were fitted by the Gaussian/Lorentzian (G/L = 4.0) distribution and Shirley background subtraction.

The surface contact angles were measured employing the sessile-drop method on a contact angle measuring system (EasyDrop Standard, KRUSS) under ambient conditions in air. Three different liquids, ultrapure water, glycerol and diiodomethane were used and the contact angles, θ, were determined by analyzing the droplet shape using the DSA1 software (KRUSS). Six contact angles were measured from each group of samples and averaged to calculate the total surface free energy, dispersive component and polar component of the two groups of samples. The dispersive component reflects the London force and is related to the morphology of the solid surface, whereas the polar component corresponds to the non-London force associated with the polarity of molecules on the surface.[22] The calculation method can be found in Ref. 23.

Protein adsorption

Adsorption of proteins on the bare and DLC-coated NiTi samples was evaluated by the micro BCA protein assay kit (Pierce). The samples with dimensions of 15 mm $\times$ 15 mm $\times$ 2 mm were ultrasonically washed in acetone, alcohol, and ultrapure water for 5 min sequentially and immersed in a phosphate buffer saline (PBS, pH = 7.4) for 30 min before incubating in 2 mL high-glucose Dulbecco's Modified Eagle's Medium (DMEM, Gbico) supplemented with 10% fetal bovine serum (FBS, Gbico) in a humidified atmosphere of 5% CO_2 at 37°C for 30, 60, and 120 min, respectively. The samples were then washed thrice carefully to remove loose proteins and then each sample was put in 2 mL of 10%

sodium dodecyl sulfate (SDS) in 12-well plates at 37°C overnight. Afterward, 100 μL of the SDS solution were loaded into 96-well plates and mixed with isometric micro BCA mixtures before incubation at 37°C for 120 min. The absorbance of each well was measured by fluorescence spectrophotometry (F-4500, HITACHI) at 562 nm and the adsorbed protein concentrations were determined from the calibration curve. Triplicate samples were measured at each time point to improve the statistics.

Leach of Ni ions

To measure the amount of Ni ions leached into the culture medium, the ultrasonically cleaned bare and DLC-coated NiTi samples with an exposed area of 5.7 cm^2 were immersed in tightly closed 10-mL polyethylene bottles containing 2 mL of DMEM supplemented with 10% FBS. They were incubated in a thermostatic chamber at 37°C ± 0.2°C for 1, 4, 7 and 10 days, respectively. After incubation, the Ni ions concentration was measured by inductively coupled plasma mass spectrometry (ICP-MS, Thermo Scientific Corp, USA). Before the measurement, the solutions were diluted 10 times. The collision and reaction cell technology as well as internal standard calibration were adopted to minimize the influence of the cell culture medium and proteins. Triplicate samples were measured at each time point and the average and standard deviation were calculated for statistical analysis. The surface morphology of the NiTi alloy and DLC-coated sample before and after immersion for 10 days was examined by field-emission scanning electron microscopy (FE-SEM, JSM-7000F) at an accelerating voltage of 20 kV.

Cell culture

The endothelial cell (EC) line was obtained from American Type Culture Collection (ATCC, CRL-2922). They have the characteristics of differentiated ECs functions such as angiogenesis, homeostasis, thrombosis, blood pressure, and inflammation and can be cultured to high passages without appreciable changes in the growth rate and phenotype, thus avoiding the diversity of primary isolates of ECs from different individuals, limitation of replication potential, as well as the senescent tendency in cultures.[24,25] The cells were cultured in high-glucose DMEM supplemented with 10% FBS and 1% (v/v) penicillin/streptomycin in 75-cm^2 tissue culture flakes and incubated in humidified atmosphere of 5% CO_2 at 37°C. Passages 3–8 were used in the experiments.

Cell adhesion, morphology, and viability

To monitor cell adhesion, the specimens were immersed in 2 mL of the cell suspension at a density of 20,000 cells mL^{-1} for 30, 60, and 120 min. At each time point, the specimens were rinsed with PBS carefully to remove loose cells and fixed in 4% paraformaldehyde for 30 min. They were then stained with 4′,6′-diamidino-2-phenylindole (DAPI) in dark for 10 min and rinsed thrice with PBS before the cell numbers were countered from six random fields using a fluorescence microscope (Nikon 80i).

The ECs were seeded at a density of 20,000 cells mL^{-1} in a complete culture medium and grown on the samples for 24 h in 12-well cell culture plates (2 mL per well). Afterward, the samples were rinsed thrice with PBS, fixed in 2.5% glutaraldehyde for 1 h, dehydrated in graded ethanol solutions (30, 60, 70, 95, and 100% v/v) for 10 min sequentially, and dried in vacuum for 24 h. The morphology of the ECs was observed by FE-SEM (JSM-7000F) at an accelerating voltage of 20 kV after the surfaces were sputter coated with a 10-nm thick platinum layer.

Cell viability was quantified using a cell counting kit-8 (CCK-8, Bestbio). Each specimen was sterilized by 75% ethanol, rinsed thrice in PBS, and placed into one well of 12-well tissue culture plates. Nearly 2 mL of the cell suspension with a density of 20,000 cells mL^{-1} was injected into each well of the culture plates and incubated for 1, 3, and 6 days. The cell culture medium was refreshed every 2–3 days depending on the color of the medium. At each time point, the specimens were rinsed thrice with PBS and transferred to fresh 12-well tissue culture plates. About 0.9 mL of the culture medium supplemented with 0.1 mL CCK-8 was injected into each well of the culture plates and incubated for 4 h. Afterward, 0.2 mL of the solution was put into a well of the 96-well plates and the absorbance was measured on a fluorescence spectrophotometer (F-4500, HITACHI) at 450 nm. Three samples of each group were averaged to improve the statistics.

Influence of Ni ions concentration on cell viability

The ECs were seeded in 12-well cell culture plates at a density of 20,000 per well and cultured in a complete medium supplemented with Ni^{2+} (in the form of $NiCl_2{\cdot}6H_2O$) at concentrations of 0, 0.1, 0.2, 0.4, and 0.8 mmol L^{-1}, respectively. The culture media were refreshed 2 or 3 days. After 7 days, the images were acquired using a biological microscope (Olympus) equipped with a digital camera in the infrared mode. Cell viability was quantified using the CCK-8 as described previously.

Thrombogenicity-related gene expressions

The expression levels of the thrombogenicity-related genes were quantitatively analyzed by the real-time polymerase chain reaction (RT-PCR). The ECs were seeded on the sample surface in 12 well plates at a density of 10,000 cells cm^{-2}. After culturing for 3 and 7 days, the total RNA was isolated using TRIzol reagent (Invitrogen) according to the manufacturer's instructions. First of all, the strand complementary DNA (cNDA) was reversed transcribed from 1 μg extracted RNA using the First Strand cDNA Synthesis Kit (ROCHE). Six genes: thrombomodulin (TM), tissue factor (TF), tissue plasminogen activator (tPA), plasminogen activator inhibitor-1 (PAI-1), von Willebrand factor (vWF), and *prostacyclin synthase* (PGIS) were selected as thrombogenicity-related genes, in which TM, tPA and PGIS were antithrombogenic whereas TF, PAI-1 and vWF were thrombogenic. The sequences of the primers for the six selected genes and housekeeping gene (β-actin) used in this study are listed in Table I. Amplification and quantification of the related genes were performed on the RT-PCR instrument (Chromo4, Bio-rad) with SYBR Green I dye (SYBR® *Premix Ex Taq*™,

TABLE I. Primers Used in Real-Time PCR of Selected Gene Transcripts

Gene	Primer Sequences	Annealing Temperature (°C)
TM	F: 5′-CTGCCGATGTCAT TTCCTTGCT-3′ R: 5′-TGTTGTCTCCCGT AACCCACTG-3′	60
TF	F: 5′-GGAACCCAAACCC GTCAATCAAG-3′ R: 5′-GGTAGGAGAAGAC CCGTGCCAAG-3′	60
tPA	F: 5′-AACCCAGATCGA GACTCAAAGC-3′ R: 5′-GACCCATTCCCA AAGTAGCAG-3′	60
PAI-1	F: 5′-GGTGCTGGTGAA TGCCCTCTAC-3′ R: 5′-GACAGTGCTGC CGTCTGATTTG-3′	60
vWF	F: 5′-AGAAACGCTCCTTCT CGATTATTG-3′ R: 5′-TGTCAAAAAATTCCCC AAGATACAC-3′	60
PGIS	F: 5′-AGGAGAAGCACGG TGACATC-3′ R: 5′-GCAGCGCCTCAAT TCCGTAA-3′	60
β-actin	F: 5′-GATCATTGCTCC TCCTGAGC-3′ R: 5′-GTCATAGTCCGC CTAGAAGCAT-3′	60

F = forward, R = reverse.

Takara). The relative expression levels were determined using the $2_{T}^{-\Delta\Delta C}$ method.[26]

Statistical analysis

Numerical data were analyzed using one-way ANOVA and present as mean ± standard deviation (SD). Results of $p < 0.05$ were considered statistical significant.

RESULTS AND DISCUSSION

Sample characterization

Figure 1 shows the microstructure and surface morphology of the samples. The Raman spectrum in Figure 1(a) discloses a wide peak between 900 and 1800 cm^{-1} that can be deconvoluted into two peaks: D and G at 1350 and 1580 cm^{-1} corresponding to the breathing mode of sp^2 C only in the rings and stretching vibration of any pair of sp^2 C in the chains or rings, respectively.[17] The HR-TEM image in Figure 1(b) reveals that the coating has a random atomic arrangement thus indicating an amorphous structure which is also confirmed by the dim halo electron diffraction pattern shown in the inset photo. The Raman spectrum and HR-TEM image indicate that the coating is amorphous diamond-like carbon. The AFM images acquired from the bare NiTi and DLC-coated samples in the contact mode exhibit significant differences as shown in Figure 1(c,d). Many fine scratches arising from mechanical polishing can be observed on the bare NiTi surface [Fig. 1(c)] but the surface of DLC-coated sample shows dense buds originating from graphitic clusters [Fig. 1(d)]. The root-mean-square roughness changes from 21.4 (bare NiT alloy) to 45.1 nm (DLC-coated NiTi alloy).

The surface elemental compositions determined by XPS are presented in Figure 2. As shown in the survey spectra in Figure 2(a), five elements, Ni, Ti, C, N, and O, are present on the surface of the bare NiTi alloy, whereas four elements, C, N, O, and Ar are detected on the DLC-coated sample. The absence of Ni on the surface of DLC-coated NiTi alloy tends to minimize the oxidation stress in the ECs.[4] The trace amount of N on both surfaces arises from surface contamination. C and O are the dominant elements on both samples as shown in Figure 2(b). A large fraction of C on the bare NiTi surface stems from surface contamination during mechanical polishing, cleaning in ethanol, or physical and chemical adsorbed CO_2, and this is consistent with previous observation.[27,28] The atomic fraction of O on the DLC surface is 15.63% because of physical and/or chemical adsorption of O_2 when exposed to air. Liu[29] and Kwok[30] have reported similar results. The high-resolution XPS spectra reveal the chemical state of each element. The chemical state of Ni [Fig. 2(c)] is mainly Ni^0 with a small amount of Ni^{2+}.[4] In contrast, Ti [Fig. 2(d)] exists mainly in the Ti^{4+} state with very little Ti^{3+} and Ti^{2+} and no Ti^0. It can be attributed to the favorable Gibbs free energy compared to Ni oxides. Because the standard Gibbs free energy (ΔG^0) of NiO, TiO_2, and TiO are −211.7, −495, and −889.5 kJ mol^{-1}, Ti oxides form preferentially to lower the free energy of the interface.[31] The O 1s spectrum [Fig. 2(e)] acquired from the NiTi alloy can be deconvoluted into three peaks. The peak at 530.5 eV is assigned to O in TiO_2 and the two high-energy peaks at 531.8 and 533.3 eV originate from O in Ti hydroxide and hydrated Ti, respectively.[32,33] Again, similar results have been obtained in other studies.[34,35] The C 1s spectrum [Fig. 2(f)] on the bare NiTi alloy comprises two peaks at 284.8 eV (C—H) and 286.5 eV (C—O) from surface contamination.[16] The N 1s peak at 400.6 eV in Figure 2(g,j) exhibits a symmetrical structure implying its organic state from organic contamination or physical adsorption. The O 1s spectrum on the DLC-coated sample [Fig. 2(h)] can be deconvoluted into three peaks, with O=O coming from physically adsorbed oxygen because of the presence of Van der Waals force and C—O and C=O coming from chemically adsorbed oxygen because of the presence of static force. As shown in Figure 2(i), four peaks can be resolved. The peaks at 284.4 and 285.3 eV represent C sp^2 and C sp^3 and the data are consistent with the Raman results. The peaks at 286.3 and 288.2 eV correspond to C=O and C—O and agree with the deconvoluted O results.

Figure 3 shows the contact angles and surface free energy of the bare and DLC-coated NiTi samples. In general, DLC coatings have smaller contact angles and higher total surface free energy, including polar and dispersive components, compared to bare NiTi alloy. The main molecular interaction is dispersive force on both of them. After a new

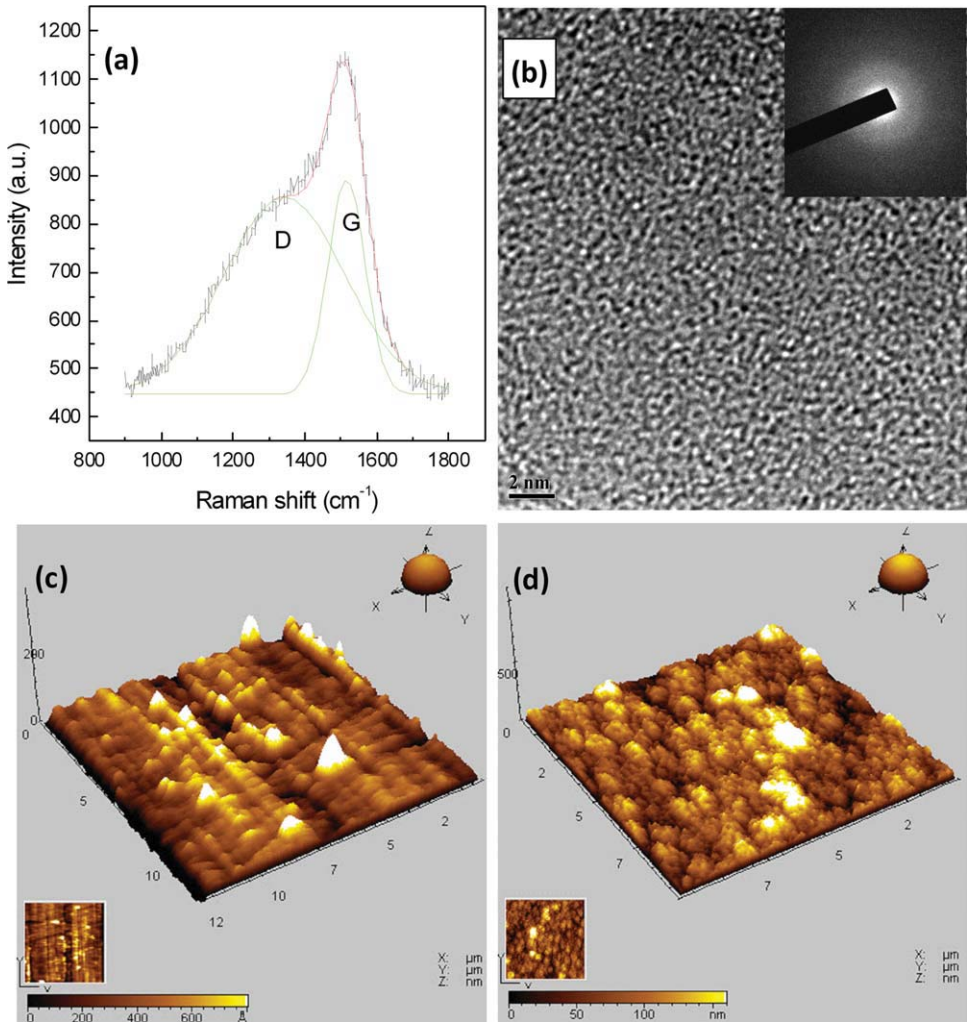

FIGURE 1. Microstructure and surface morphology of samples: (a) Raman spectrum of DLC coatings, (b) HR-TEM image and the corresponding electron diffraction pattern of DLC coatings, (c) AFM image of the bare NiTi alloy, and (d) AFM image of the DLC-coated sample. [Color figure can be viewed in the online issue, which is available at wileyonlinelibrary.com.]

surface is formed, various molecules adsorb physically and/or chemically to lower the surface free energy. The XPS results in Figure 2 reveal both physical and chemical adsorption, which alters the surface chemistry to become more stable. Because of the roughness on both surfaces, contact angle hysteresis is expected and as the surface roughness increases, the hysteresis increases.[36] The surface roughness of the bare NiTi alloy is 21.4 and 45.1 nm for DLC and so the hysteresis on DLC is expected to bigger than that on the bare NiTi alloy. Nonetheless, in general the roughness has a nanoscale and so the hysteresis can usually be ignored.

Protein adsorption

The protein adsorption values with time from the DMEM supplemented with 10% FBS on the bare and DLC-coated specimens are presented in Figure 4. After 30 min, that on the bare NiTi alloy is 0.4 μg cm^{-2}, which is higher than that on the DLC-coated sample (0.33 μg cm^{-2}). As time elapses, the increase in adsorption is quite small, indicating levelling off of protein adsorption after 30 min. In contact with a body fluid containing soluble proteins such as blood and cell culture media, proteins adsorb onto the surface of the materials very quickly driven by thermodynamics. Because there are a lot of nanoscale constituents in tissues, biomaterials possessing a nanostructured surface topography are biologically inspired materials which can effectively interact with proteins to increase bone cell functions, regeneration of vascular tissues, and so on.[37,38] The surface nanotopography may change the localized surface chemistry, restrict protein exchange, and influence the geometrical packing of proteins.[39] It has been reported that a nanostructured surface preferentially adsorb vitronectin and fibronectin to expose more amino acid sequences (such as RGD) which can promote cell adhesion.[37] As shown in Figure 1(c,d), the DLC-coated NiTi alloy has more nanoscale features than the bare NiTi alloy and may interact with some proteins more effectively to promote EC adhesion and viability. The surface energy which is another aspect that influences adsorption is intertwined with the surface morphology. Increase in the

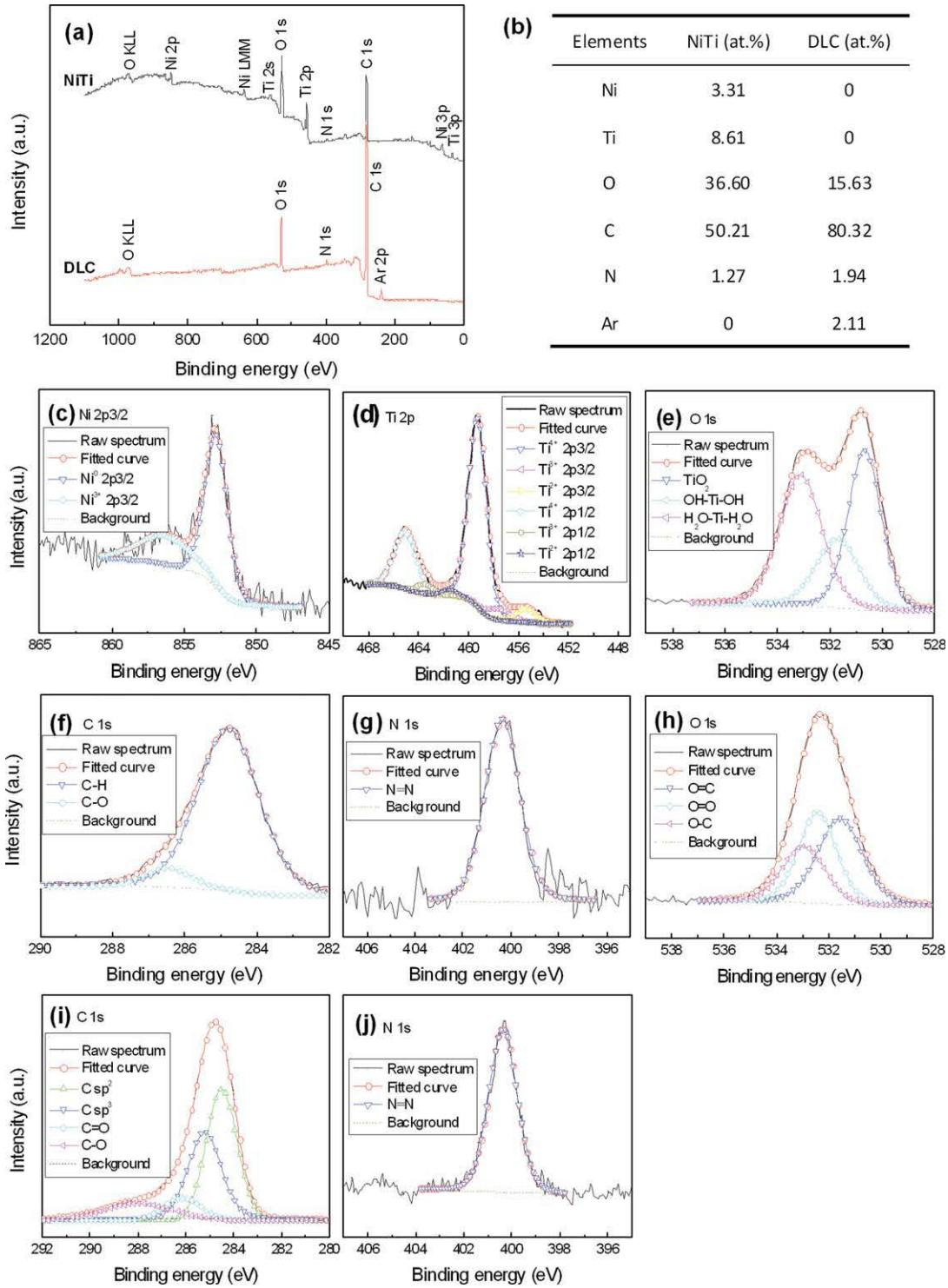

Elements	NiTi (at.%)	DLC (at.%)
Ni	3.31	0
Ti	8.61	0
O	36.60	15.63
C	50.21	80.32
N	1.27	1.94
Ar	0	2.11

FIGURE 2. Surface elemental compositions of mechanically polished NiTi and DLC-coated samples: (a) XPS survey spectra, (b) Surface elemental composition, (c–g) high-resolution XPS spectra of surface elements on the bare NiTi, and (h–j) High-resolution XPS spectra of surface elements on the DLC-coated NiTi alloy. [Color figure can be viewed in the online issue, which is available at wileyonlinelibrary.com.]

surface roughness promotes the dispersive components of the total surface energy. A hydrophilic surface tends to adsorb less protein than a hydrophobic surface,[40] and a similar trend is observed here. Popov et al.[41] have reported that for diamond/amorphous carbon composite films, a high ratio of γ_s^p (polar component) to γ_s^d (dispersive component) corresponds to a high adsorption ratio of albumin to fibrinogen thus indicative of good hemocompatibility. García and coworkers have revealed that a neutral and hydrophilic surface preferentially exposes integrin-binding domain of

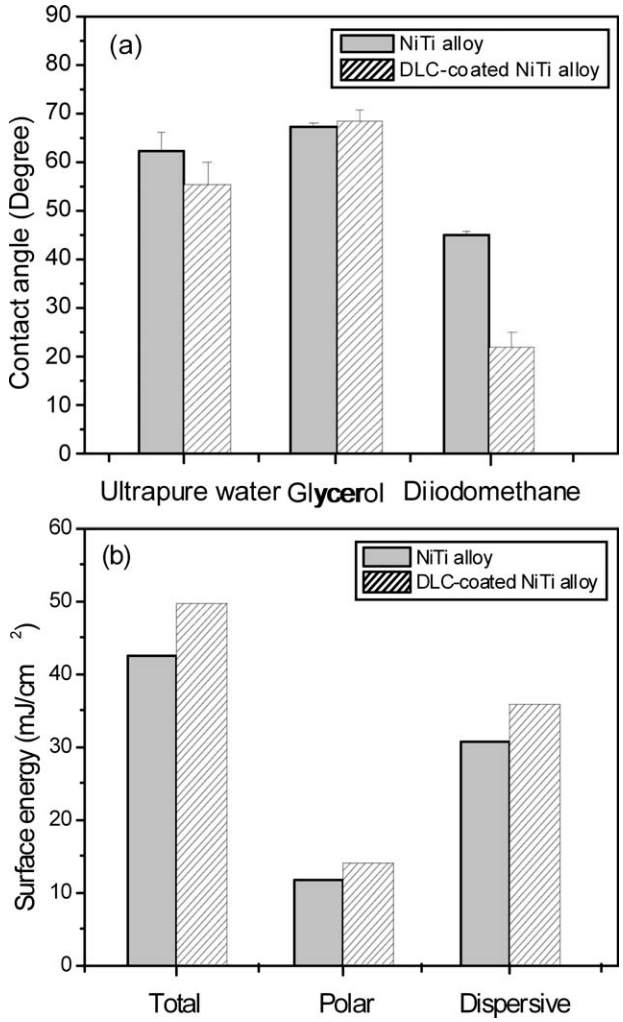

FIGURE 3. Contact angles and surface free energy of bare and DLC-coated NiTi alloy.

adsorbed fibronectin and modulates the functions of integrins and subsequent cell biological response.[42,43] Surface chemistry is also very important for protein adsorption and is closely related to the surface free energy. It can influence the amount, types, and conformation of adsorbed proteins as well as subsequent cell functions.[44–46]

Nickel ions release

Figure 5 shows the Ni ion concentrations leached from the bare and DLC-coated NiTi samples for different immersion time and surface morphology. The Ni ion concentrations released from the bare NiTi alloy increase with immersion time and are much higher than those leached from the DLC-coated one. The surface morphology in Figure 5(b) may explain this phenomenon. The native oxide film on the bare NiTi surface can increase from a few nanometers to tens of nanometers with longer immersion time, but destructive pitting corrosion occurs because of breakdown of the native oxide film. Carcinogenic Ni ions leached from the materials may bind with serum proteins thus mediating the cell behavior and functions.[47] In comparison, no appreciable morphological difference can be observed from the DLC-coated sample before and after immersion, indicating good corrosion resistance and less Ni ions out-diffusion.

Cell adhesion, morphology, viability, and gene expression

As aforementioned, the surface properties can mediate the type, number, and conformation of adsorbed proteins and consequently, the adsorbed proteins can translate the surface information into biological language to influence cell response. Figure 6 illustrates the cell adhesion, viability, and morphology on the bare and DLC-coated NiTi alloy. As shown in Figure 6(a), the adherent cell number increases with time and there are more cells on the DLC-coated NiTi alloy. For most cell types such as ECs, adhesion is essential to survival. In the adhesion process, the cells recognize the specific ligands on the adsorbed proteins (such as RGD amino acid sequence) by the integrin receptors on the cell membranes. The integrin consists of both transmembranes α and β subunits, which can pass information intra- and extra-cellularly to regulate cell adhesion, viability, morphology, and so on.[48] There are three main adhesive interactions between cells and biomaterials, focal adhesion, close contact, and extracellular matrix contact, among which focal adhesion has the shortest distance (10–20 nm) between the cells and implants thus having the strongest adhesive force.[37] The surface chemistry, energy, and topography may influence the formation, structure, composition, and area of focal adhesion through changing integrins expression and binding.[42,49,50] Neutral and hydrophilic surfaces can accelerate the formation of focal adhesion and subsequent cell adhesion.[37] The cell morphology after seeding for 24 h is depicted in Figure 6(b). The cells on NiTi alloy have spread and cobblestone appearance, while present elongated morphologies on DLC-coated one. It has been reported that elongated ECs can contribute to the cell viability and

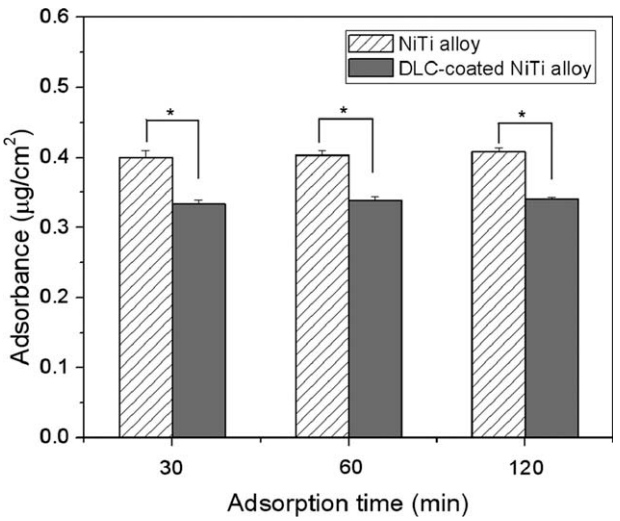

FIGURE 4. Protein adsorbance in DMEM supplemented with 10% FBS on bare and DLC-coated NiTi alloy for different adsorption time. The statistical significance is indicated by * ($p < 0.05$), $n = 3$.

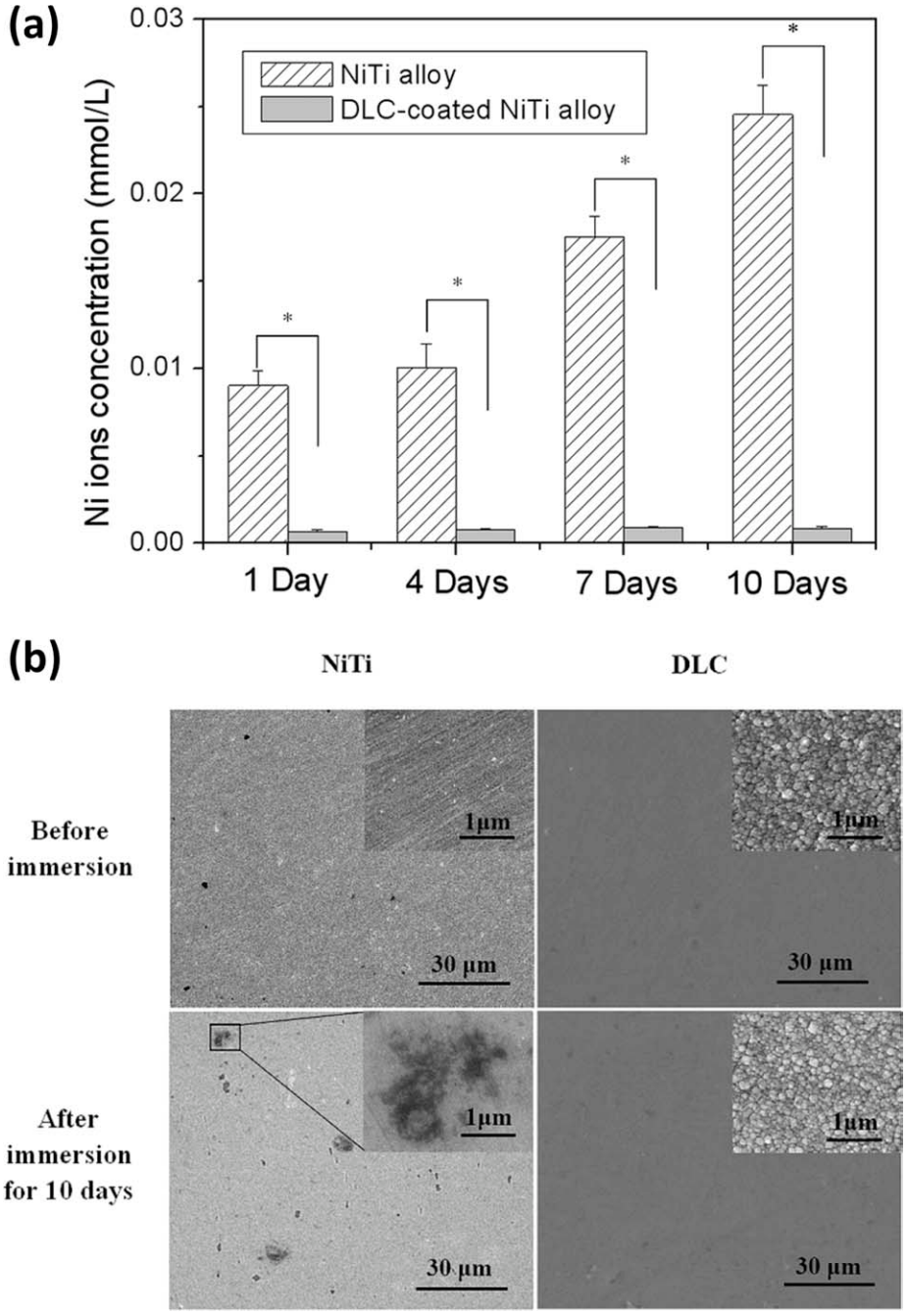

FIGURE 5. Ni ions concentration (a) and surface morphology (b) of bare and DLC-coated NiTi alloy for different immersion time. The statistical significance is indicated by * ($p < 0.001$), $n = 3$.

secretion of extracellular matrix[51] and have higher migration speeds.[52] These factors may contribute to endothelialization after device implantation. Figure 6(c) displays the cell viability at different days. It has been reported that cell communication plays an important role in cell viability[53] and so the depressed cell communication induced by the low cell population and abnormal morphology may be partially responsible for the lower cell viability on the bare NiTi alloy. The large amount of toxic Ni ions in the culture medium may also contribute to the depressed cell viability and this issue will be discussed later.

Figure 7 shows the EC morphology and viability at different Ni ions concentrations after culturing for 7 days. As shown in Figure 7(a), the cell morphology shows no obvious difference until the Ni concentration reaches 0.8 mmol L^{-1}. As the concentration increases further, the living cell number decreases and the dead cell number increases as consistent with the cell viability results in Figure 7(b). Lü et al.[13,54] have reported that a low Ni ion concentration (0.1 mmol L^{-1}) has little influence on the cell morphology and viability, but the gene expression is dramatically altered after culturing for 12 h. Hence, genotoxicity is

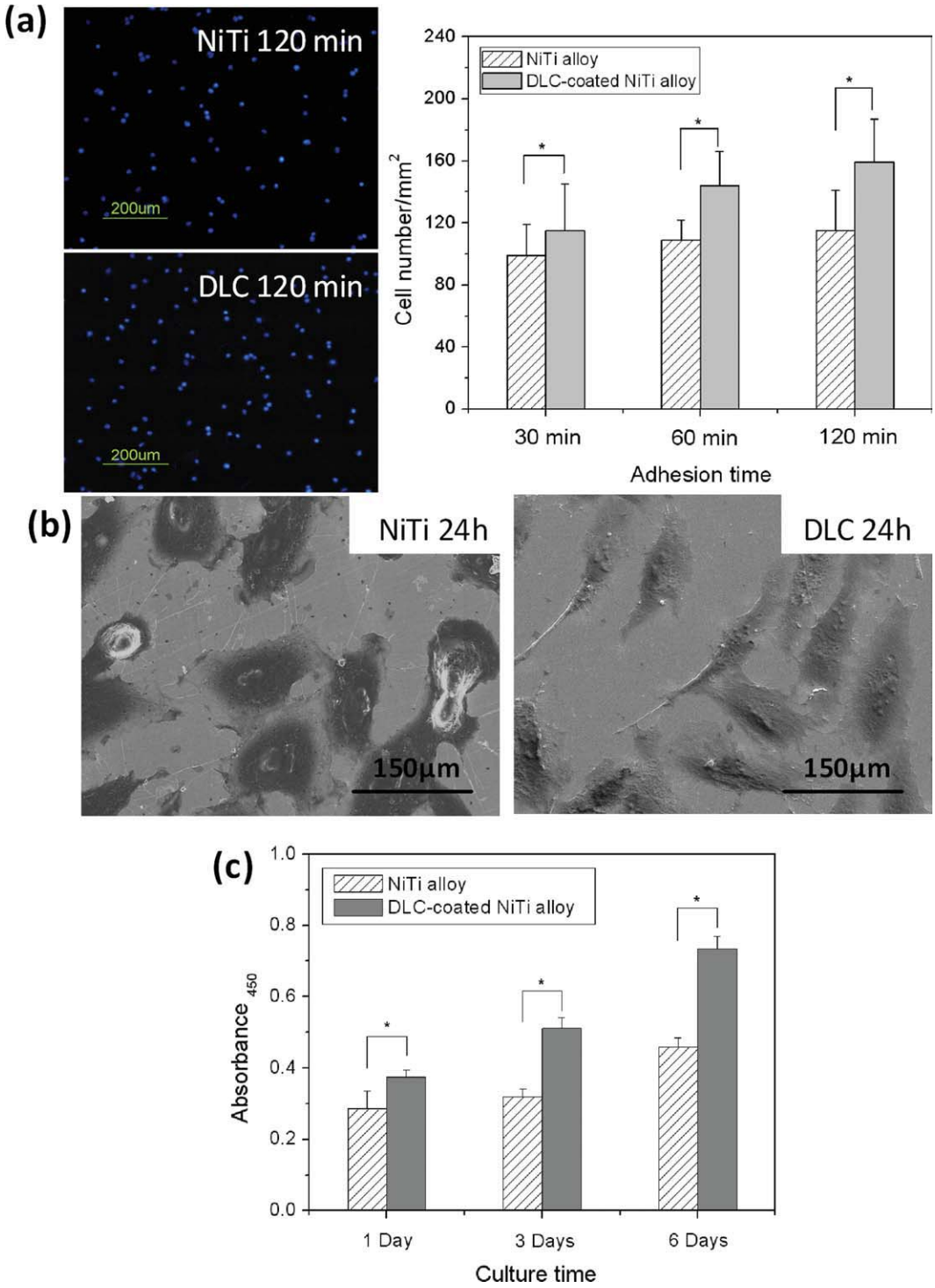

FIGURE 6. Adhesion (a), morphology (b), and viability (c) of endothelial cells on bare NiTi alloy and DLC-coated one. The statistical significance is indicated by *($p < 0.05$), $n = 3$. [Color figure can be viewed in the online issue, which is available at wileyonlinelibrary.com.]

more sensitive than cytotoxicity. Furthermore, Ni ions may influence cell viability by altering the expression levels of six related genes in the cell cycle pathway.[54] According to Figure 5(a), the Ni ion concentration leached from the bare NiTi alloy after immersion for 10 days is 0.0255 mmol L^{-1} that is below 0.8 mmol L^{-1} at which cell viability is depressed seriously. Hence, the leached Ni ions should have little effects on cytotoxicity but the associated genotoxicity needs to be studied in more details.

The expression levels of thrombogenicity-related gene of the ECs cultured on the bare and DLC-coated samples for 3 and 7 days are presented as histograms in Figure 8. The TF, TM, tPA, vWF, and PGIS after incubation for 3 days and tPA, vWF, PGIS after incubation for 7 days show no significant

difference. The expression of PAI-1 is promoted on the DLC surface regardless of culturing time and the expression of TF and TM on the DLC are upregulated after incubation for 7 days. The influence of the biomaterials on EC thrombogenicity is still a controversial issue. Some researchers have suggested that the substrate has no effects, while others consider it to be influential.[1] Nonetheless, the leached ions from the materials due to the spontaneous electrochemical process during culturing may influence the gene expression. The Ni ion concentration in the culture medium of the bare NiTi alloy is significantly higher than that of the DLC-coated alloy as shown in Figure 5(a). It may change the gene expression levels and induce cell dysfunction. It has been reported that Ni ions can influence gene expression and cell functions.[13] However, the dose, time, and underlying molecular mechanism are not clear and further studies on the effects of Ni on gene expression of ECs will be insightful.

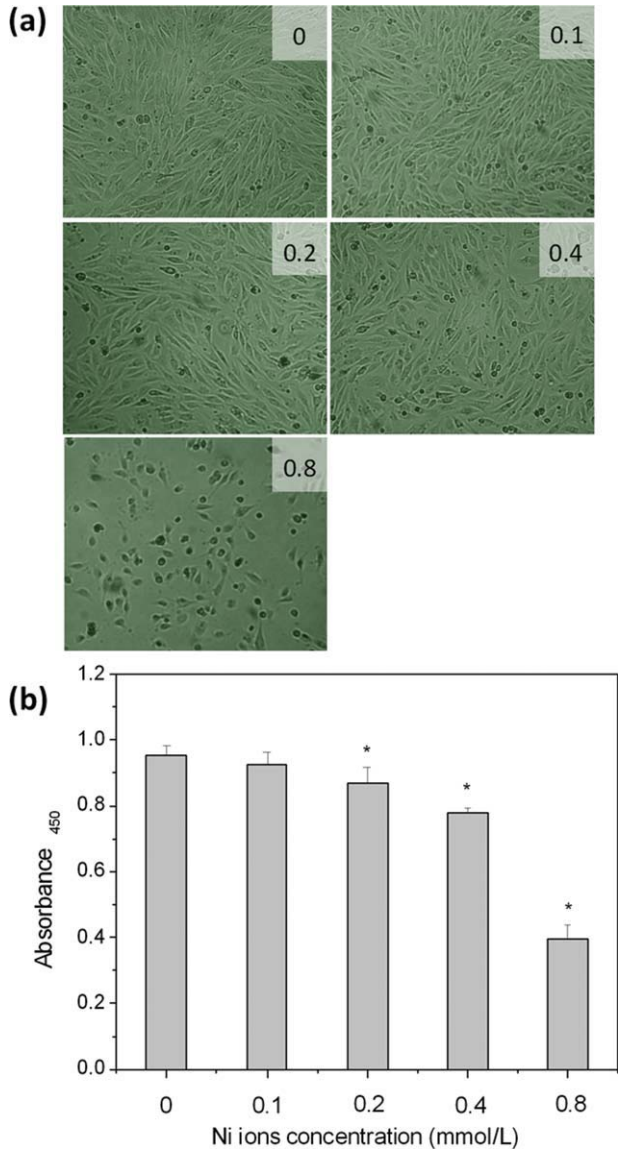

FIGURE 7. Endothelial cells morphology (a) and viability (b) at different Ni ion concentrations after seeding for 7 days. The statistical significance is indicated by $*p < 0.05$ ($n = 3$) versus the sample without exposure to Ni ions. [Color figure can be viewed in the online issue, which is available at wileyonlinelibrary.com.]

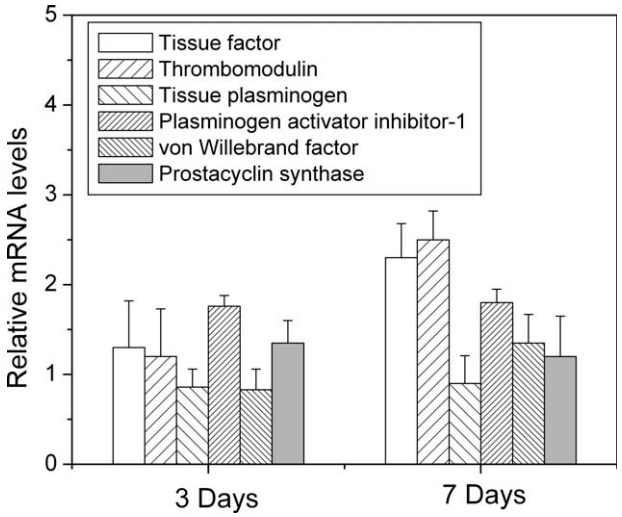

FIGURE 8. RT-PCR results of selected genes at days 3 and 7. The expression levels of genes of interest are normalized to the housekeeping gene β-actin and analyzed using the $2_T^{-\Delta\Delta C}$ method, where $\Delta\Delta C_T = \Delta C_T$ (DLC) $- \Delta C_T$ (NiTi).

CONCLUSION

Diamond-like carbon (DLC) coatings with a nanoscale surface have been fabricated on NiTi alloy using arc-enhanced magnetron sputtering. The results show that the adhesion, morphology, and viability of endothelial cells (ECs) on the DLC coatings are better than that on bare NiTi alloy. The ease to adhere, elongated morphology, and high viability of ECs on DLC coatings lead to faster endothelialization compared to bare NiTi alloy after surgical implantation. The DLC coatings reduce out-diffusion of deleterious Ni ions from the materials, but the release of a trace amount of Ni ions from the bare NiTi alloy has little influence on the morphology and cell viability in the short term. The enhanced biological response of the ECs to DLC coatings depends on the surface properties and the long-term effects require further study. The expression levels of thrombogenicity-related genes are similar possibly because the ECs are in an inactivated state thus exhibiting the non-thrombogenic phonotype. Our results suggest that DLC coatings are promising in surface modification of NiTi alloy in cardiovascular applications.

REFERENCES

1. McGuigan AP, Sefton MV. The influence of biomaterials on endothelial cell thrombogenicity. Biomaterials 2007;28:2547–2571.
2. Gonzales C, Pedrazzini T. Progenitor cell therapy for heart disease. Exp Cell Res 2009;315:3077–3085.
3. Burt HM, Hunter WL. Drug-eluting stents: A multidisciplinary success story. Adv Drug Deliv Rev 2006;58:350–357.
4. Plant SD, Grant DM, Leach L. Behavior of human endothelial cells on surface modified NiTi alloy. Biomaterials 2005;26:5359–5367.
5. Finn A, Nakazawa G, Joner M, Kolodgie F, Mont E, Gold H. Vascular responses to drug-eluting stents: Importance of delayed healing. Arterioscl Thromb Vasc 2007;27:1500–1510.
6. Lagerqvist B, James S, Stenestrand U, Lindbäck J, Nilsson T, Wallentin L. Long-term outcomes with drug-eluting stents versus bare-metal stents in Sweden. N Eng J Med 2007;356:1009–1019.

7. Samaroo HD, Lu J, Webster TJ. Enhanced endothelia cell density on NiTi surfaces with sub-micron to nanometer roughness. Int J Nanomed 2008;3:75–82.
8. Castleman LS, Motzkin SM, Alicandri FP, Bonawit VL, Johnson AA. Biocompatibility of Nitinol alloy as an implant materials. J Biomed Mater Res 1976;10:695–731.
9. Sui JH, Cai W. Effect of diamond-like carbon (DLC) on the properties of the NiTi alloys. Diam Relat Mater 2006;15:1720–1726.
10. Kobayashi S, Ohgoe Y, Ozeki K, Sato K, Sumiya T, Hirakuri KK, Aoki H. Diamond-like carbon coatings on orthodontic archwires. Diam Relat Mater 2005;14:1094–1097.
11. Clarke B, Carroll W, Rochev Y, Hynes M, Bradley D, Plumley D. Influence of Nitinol wire surface treatment on oxide thickness and composition and its subsequent effect on corrosion resistance and nickel ion release. J Biomed Mater Res A 2006;79:61–70.
12. Ryhänen J. Biocompatibility evaluation of nickel-titanium shape memory metal alloy. Doctoral Thesis, Oulu University; 1999
13. Lü XY, Bao X, Huang Y, Qu YH, Lu HQ, Lu ZH. Mechanisms of cytotoxicity of nickel ions based on gene expression profiles. Biomaterials 2009;30:141–148.
14. Firstov GS, Vitchev RG, Kumar H, Blanpain B, Humbeeck JV. Surface oxidation of NiTi shape memory alloy. Biomaterials 2002;23:4863–4871.
15. Chu CL, Hu T, Wu SL, Dong YS, Yin LH, Pu YP, Lin PH, Chung CY, Yeung KWK, Chu PK. Surface structure and properties of biomedical NiTi shape memory alloy after Fenton's oxidation. Acta Biomater 2007;3:795–806.
16. Shabalovskaya SA, Tian H, Anderegg JW, Schryvers DU, Carroll WU, Humbeeck JV. The influence of surface oxides on the distribution and release of nickel from Nitinol wires. Biomaterials 2009;30:468–477.
17. Chu PK, Li LH. Characterization of amorphous and nanocrystalline carbon films. Mater Chem Phys 2006;96:253–277.
18. Takeno T, Shiota H, Sugawara T, Miki H, Takagi T. Highly adherent tungsten-containing diamond-like carbon (W-DLC) coating on a NiTi shape memory alloy under 10% tensile strain. Diam Relat Mater 2009;18:403–406.
19. Poon RWY, Yeung KWK, Liu XY, Chu PK, Chung CY, Lu WW, Cheung KMC, Chan D. Carbon plasma immersion ion implantation of nickel-titanium shape memory alloys. Biomaterials 2005; 26:2265–2272.
20. Kobayashi S, Ohgoe Y, Ozeki K, Sato K, Sumiya T, Hirakuri KK, Aoki H. Diamond-like carbon coatings on orthodontic archwires. Diam Relat Mater 2005;14:1094–1097.
21. Sui JH, Gao ZY, Cai W, Zhang ZG. Corrosion behavior of NiTi alloys coated with diamond-like carbon (DLC) fabricated by plasma immersion ion implantation and deposition. Mater Sci Eng A 2007;452/453:518–523.
22. Zhao Q, Liu Y, Abel EW. Effect of temperature on the surface free energy of amorphous carbon films. J Colloid Interf Sci 2004;280:174–183.
23. Zhao LZ, Wei YP, Li JX, Han Y, Ye RD, Zhang YM. Initial osteoblast functions on Ti-5Zr-3Sn-5Mo-15Nb titanium alloy surfaces modified by microarc oxidation. J Biomed Mater Res A 2010;92:432–440.
24. Edgell CJ, McDonald CC, Graham JB. Permanent cell line expressing human factor VIII-related antigen established by hybridization. Proc Natl Acad Sci USA 1983;80:3734–3737.
25. Rieber AJ, Marr HS, Comer MB, Edgell CJ. Extent of differentiated gene expression in the human endothelium-derived EA.hy926 cell line. Thromb Haemost 1993;69:476–480.
26. Livak KJ, Schmittgen TD. Analysis of relative gene expression data using real-time quantitative PCR and the $2_T^{-\Delta\Delta C}$ method. Methods 2001;25:402–408.
27. Wong MH, Cheng FT, Pang GKH, Man HC. Characterization of oxide film formed on NiTi by laser oxidation. Mater Sci Eng A 2007; 448:97–103.
28. Tan L, Crone WC. Surface characterization of NiTi modified by plasma source ion implantation. Acta Mater 2002;50:4449–4460.
29. Liu C, Li GQ, Chen WW, Mu ZX, Zhang CW, Wang L. The study of doped DLC films by Ti ion implantation. Thin Solid Films 2005; 475:279–282.
30. Kwok SCH, Wang J, Chu PK. Surface energy, wettability, and blood compatibility phosphorus doped diamond-like carbon films. Diam Relat Mater 2005;14:78–85.
31. Shabalovskaya SA, Rondelli GC, Undisz AL, Anderegg JW, Burleigh TD, Rettenmayr ME. The electrochemical characteristics of native Nitinol surfaces. Biomaterials 2009;30:3662–3671.
32. Frateur I, Lecoeur J, Zanna S, Olsson CA, Landolt D, Marcus P. Adsorption of BSA on passivated chromium studied by a flow-well EQCM and XPS. Electrochim Acta 2007;52:7660–7669.
33. Shabalovskaya SA. Surface, corrosion and biocompatibility aspects of Nitinol as an implant material. Biomed Mater Eng 2002;12:69–109.
34. Chu CL, Hu T, Wu SL, Dong YS, Yin LH, Pu YP, Lin PH, Chung CY, Yeung KK, Chu PK. Surface structure and properties of biomedical NiTi shape memory alloy after Fenton's oxidation. Acta Biomater 2007;3:795–806.
35. Green SM, Grant DM, Wood JV. XPS characterization of surface modified Ni-Ti shape memory alloy. Mater Sci Eng A 1997;224: 21–26.
36. Quéré D. Wetting and roughness. Annu Rev Mater Res 2008;38: 71–99.
37. Narayan R. Biomedical Materials. New York: Springer Press; 2009. p 215–260.
38. Liu XY, Chu PK, Ding CX. Surface nano-functionalization of biomaterials. Mater Sci Eng R 2010;70:275–302.
39. Lord MS, Foss M, Besenbacher F. Influence of nanoscale surface topography on protein adsorption and cellular response. Nano Today 2010;5:66–78.
40. Janocha B, Hegemann D, Oehr C, Brunner H, Rupp F, Gerstorfer JG. Adsorption of protein on plasma-polysiloxane layers of different surface energies. Surf Coat Technol 2001;142–144:1051–1055.
41. Popov C, Vasilchina H, Kulisch W, Danneil F, Stüber M, Ulrich S, Welle A, Reithmaier JP. Wettability and protein adsorption on ultrananocrystalline diamond/amorphous carbon composite films. Diam Relat Mater 2009;18:895–898.
42. Keselowsky BG, Collard DM, García AJ. Surface chemistry modulates focal adhesion composition and signaling through changes in integrin binding. Biomaterials 2004;25:5947–5954.
43. Keselowsky BG, Collard DM, García AJ. Surface chemistry modulates fibronectin conformation and directs integrin binding and specificity to control cell adhesion. J Biomed Mater Res A 2003; 66:247–259.
44. Michael KE, Vernekar VN, Keselowsky BG, Meredith JC, Latour RA, García AJ. Adsorption-induced conformational changes in fibronectin due to interactions with welldefined surface chemistries. Langmuir 2003;19:8033–8040.
45. Kowalczynska HM, Nowak-Wyrzykowska M, Dobkowski J, Kolos R, Kaminski J, Makowska-Cynka A, Marciniak E. Adsorption characteristics of human plasma fibronectin in relationship to cell adhesion. J Biomed Mater Res A 2002;61:260–269.
46. Shen M, Horbett TA. The effects of surface chemistry and adsorbed proteins on monocyte/macrophage adhesion to chemically modified polystyrene surfaces. J Biomed Mater Res A 2001; 57:336–345.
47. Hang RQ, Ma SL, Ji V, Chu PK. Corrosion behavior of NiTi alloy in fetal bovine serum. Electrochim Acta 2010;55:5551–5560.
48. Siebers MC, Brugge PJ, Walboomers XF, Jansen JA. Integrins as linker proteins between osteoblasts and bone replacing materials. A critical review. Biomaterials 2005;26:137–146.
49. Miyauchi T, Yamada M, Yamamoto A, Iwasa F, Suzawa T, Kamijo R, Baba K, Ogawa T. The enhanced characteristics of osteoblast adhesion to photofunctionalized nanoscale TiO_2 layers on biomaterials surfaces. Biomaterials 2010;31:3827–3839.
50. Lim JY, Dreiss AD, Zhou ZY, Hansen JC, Siedlecki CA, Hengstebeck RW, Cheng J, Winograd N, Donahue HJ. The regulation of integrin-mediated osteoblast focal adhesion and focal adhesion kinase expression by nanoscale topography. Biomaterials 2007; 28:1787–1797.
51. Masaru T, Aiko T, Emiko I, Hiroshi S, Sadaaki Y, Masatsugu S. Effect of pore size of self-organized honeycomb-patterned polymer films on spreading, focal adhesion, proliferation, and function of endothelial cells. J Nanosci Nanotechnol 2007;7:763–772.
52. McGrath JL, Osborn EA, Tardy YS, Dewey CF, Hartwig JH. Regulation of the actin cycle in vivo by actin filament severing. Proc Natl Acad Sci USA 2000;97:6532–6537.
53. Civitelli R. Cell-cell communication in the osteoblast/osteocyte lineage. Arch Biochem Biophys 2008;473:188–192.
54. Lü XY, Lu HQ, Zhao LF, Yang YM, Lu ZH. Genome-wide pathways analysis of nickel ion-induced differential genes expression in fibroblasts. Biomaterials 2010;31:1965–1973.